Structural Chemistry and Magnetic Properties of Incommensurate $Sr_{1+x}(Co_xMn_{1-x})O_3$

Nicola A. Jordan,[†] Peter D. Battle,*[,†] Sander van Smaalen,[‡] and Markus Wunschel[‡]

Inorganic Chemistry Laboratory, Oxford University, South Parks Road, Oxford, OX1 3QR, U.K., and Laboratory of Crystallography, University of Bayreuth, 95440 Bayreuth, Germany

Received June 12, 2003. Revised Manuscript Received August 14, 2003

The incommensurate, modulated crystal structures of $Sr_{1+x}(Co_xMn_{1-x})O_3$ ($x \approx 0.266$ and 0.280) have been refined by a (3+1)D superspace profile analysis of neutron powder diffraction data. The structures are related to the 2H perovskite structure and consist of two subsystems, $[Co_xMn_{1-x}O_3]_\infty$ chains containing face-sharing MnO_6 octahedra and CoO_6 trigonal prisms (albeit with some cation site inversion), separated from each other by $[Sr]_\infty$ chains. The observed structures are closely related to those expected for the idealized compositions $Sr_{14}Co_3Mn_8O_{33}$ and $Sr_9Co_2Mn_5O_{21}$. Both of the compositions investigated show hysteresis in their magnetic behavior below 13 K.

Introduction

The perovskite structure has occupied a central position in solid-state chemistry for many years. This can be attributed, in part, to the ability of the structure to accommodate a wide range of metallic elements in a wide range of oxidation states. The flexibility in the cation content stems from the abilities of the structure to exist in both pseudo-cubic and hexagonal forms, and to compensate for changes in the cation oxidation state by allowing a significant (≤17%) vacancy concentration on the anion sublattice. Thus, $SrCoO_3$ and $SrCoO_{2.5}$ (or $Sr_2Co_2O_5$) can both be prepared, albeit under different conditions of temperature and $p(O_2)$. These perovskite-related materials both adopt pseudo-cubic structures, in contrast to $SrMnO_3$ which adopts a hexagonal structure. It has been established that the stoichiometry and structure of perovskites control their electronic properties, thus at low temperatures $SrCoO_3$ is a metallic ferromagnet, whereas $SrCoO_{2.5}$ and $SrMnO_3$ are insulating antiferromagnets. Some years ago it was recognized[1] that this raises an interesting question concerning the variations in structure and magnetic behavior which occur as the Mn/Co ratio and oxygen stoichiometry vary in the system $SrCo_{1-x}Mn_xO_{3-\delta}$. A study by X-ray powder diffraction and EXAFS apparently revealed three new phases in the composition range $0 \le x \le 1$, the most interesting being an incommensurate phase ($0.4 < x < 0.55$) which was thought to be related structurally to the hexagonal perovskites, although EXAFS revealed an intercation distance of ~2.8 Å which is not normally found in those structures. Furthermore, the similarity of the EXAFS data collected on samples in the composition range $0.8 < x < 1$ to those collected on both the new incommensurate phase and what was widely described at the time as the hexagonal (H) form of $SrCoO_{2.5}$ led to the suggestion that H−$Sr_2Co_2O_5$ might also be part of an incommensurate system. This phase had been studied in some depth,[2−5] but the X-ray powder diffraction pattern had not been indexed in a satisfactory way.

Many of the ambiguities concerning H−$Sr_2Co_2O_5$ have been resolved in recent years. Harrison et al.[6] used single-crystal X-ray diffraction to show that the phase actually has the composition $Sr_6Co_5O_{15}$. The structure is indeed related to that of the 2H hexagonal perovskites (for example[7] $BaMnO_3$) but the chains of transition metal polyhedra parallel to [001] consist not just of CoO_6 octahedral, but of an ordered 4:1 sequence of octahedra and trigonal prisms. The phase is thus the $n = 1$ member of the structural family $A_{3n+3}A'_nB_{n+3}O_{6n+9}$ (A = Sr, A′ = Co (prism), B = Co (octahedron)) first described by Darriet and Subramanian.[8] It has since been shown that the full extent of this family is better appreciated when the formulation $A_{1+x}(A'_xB_{1-x})O_3$ is used, and an elegant analysis by Perez-Mato et al[9] has shown that the family members can be considered to adopt commensurate or incommensurate modulated structures, thus lending support to the suggestion made previously.[1] A model has been produced[9,10] which fa-

* To whom correspondence should be addressed. E-mail: peter.battle@chem.ox.ac.uk.
[†] Oxford University.
[‡] University of Bayreuth.

(1) Battle, P. D.; Gibb, T. C.; Strange, R. *J. Solid State Chem.* **1989**, *81*, 217.
(2) Grenier, J.-C.; Ghodbane, S.; Demazeau, G. *Mater. Res. Bull.* **1979**, *14*, 831.
(3) Grenier, J.-C.; Fournès, L.; Pouchard, M.; Hagenmuller, P. *Mater. Res. Bull.* **1986**, *21*, 441.
(4) Rodriguez, J.; Gonzalez-Calbet, J. M.; Grenier, J. C.; Pannetier, J.; Anne, M. *Solid State Commun.* **1987**, *62*, 231.
(5) Rodríguez, J.; González-Calbet, J. M. *Mater. Res. Bull.* **1986**, *21*, 429.
(6) Harrison, W. T. A.; Hegwood, S. L.; Jacobson, A. J. *J. Chem. Soc., Chem. Commun.* **1995**, 1953.
(7) Cussen, E. J.; Battle, P. D. *Chem. Mater.* **2000**, *12*, 831.
(8) Darriet, J.; Subramanian, M. A. *J. Mater. Chem.* **1995**, *5*, 543.
(9) Perez-Mato, J. M.; Zakhour-Nakhl, M.; Weill, F.; Darriet, J. *J. Mater. Chem.* **1999**, *9*, 2795.
(10) Evain, M.; Boucher, F.; Gourdon, O.; Petricek, V.; Dusek, M.; Bezdicka, P. *Chem. Mater.* **1998**, *10*, 3068.

10.1021/cm031096+ CCC: $25.00
Published on Web 10/04/2003

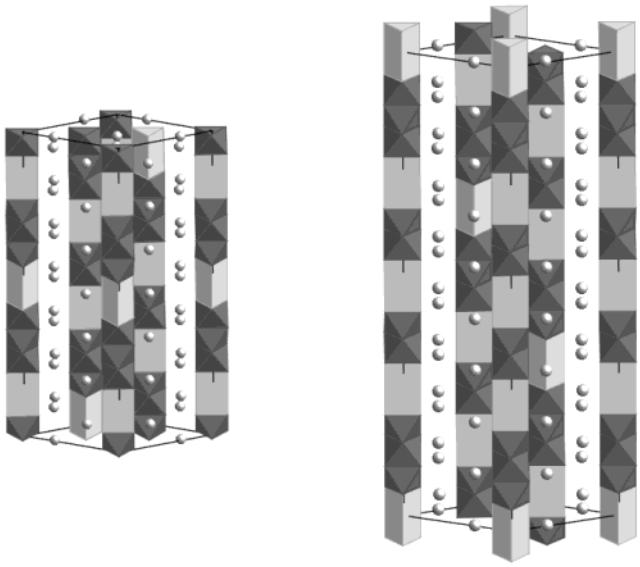

Figure 1. Polyhedral representation of the idealized crystal structures of $Sr_{14}Co_3Mn_8O_{33}$ and $Sr_9Co_2Mn_5O_{21}$.

cilitates the description of these structures in (3+1)-dimensional ((3+1)D) space; this approach is necessary in the case of incommensurate phases and helpful in the remainder because it reduces the number of adjustable parameters needed to define the structure.

Developments in our understanding of structural chemistry have thus provided a framework within which the behavior of "H−$Sr_2Co_2O_5$" can be understood, and several related compounds, including $Sr_{14/11}CoO_3$, have now been studied by single-crystal X-ray diffraction using the superspace approach.[10−14] Furthermore, developments in computer software[15,16] have made it possible to analyze modulated crystal structures in superspace using powder diffraction data.[17] We have therefore returned to the Sr−Co−Mn−O system which was previously recognized as being incommensurate but which could not be fully characterized when it was first synthesized. On the basis of results of the earlier study and on the work of Blake et al,[18] we have prepared samples with the nominal compositions $Sr_{14}Co_3Mn_8O_{33}$ and $Sr_9Co_2Mn_5O_{21}$, that is the $A_{1+x}(A'_xB_{1-x})O_3$ phases with $x = 3/11$ and $2/7$ respectively; their ideal, commensurate crystal structures are drawn in Figure 1. We describe herein a superspace analysis of their crystal structures based on both X-ray and neutron powder diffraction data, the latter being used to investigate the ordering of the Co and Mn cations over the octahedral and prismatic sites in the two compositions selected for study. We also briefly describe the magnetic behavior of these samples.

Experimental Section

The samples having nominal compositions $Sr_{14}Co_3Mn_8O_{33}$ and $Sr_9Co_2Mn_5O_{21}$ will be referred to as P and Q, respectively. Polycrystalline samples (~6 g) were prepared by the ceramic method. Stoichiometric quantities of $SrCO_3$, Co_3O_4, and MnO_2 were ground together and reacted in alumina crucibles for 24 h at 800 °C before being pelletized and heated at 1200 °C for 4 d (P) or 7 d (Q) with intermittent regrinding. X-ray powder diffraction patterns of the final products were recorded using Cu $K\alpha_1$ radiation on a Siemens D5000 diffractometer operating at room temperature in Bragg−Brentano geometry over the angular range $10 \le 2\theta/° \le 100$ with a step size $\Delta 2\theta = 0.02°$. Neutron diffraction data were collected, also at room temperature, over the angular range $5 \le 2\theta/° \le 145$ ($\Delta 2\theta = 0.05°$) at a wavelength of 1.59573(5) Å on the diffractometer D2b at ILL Grenoble; the samples were mounted in vanadium cans of 8-mm diam. All the diffraction data were analyzed by Rietveld-style[19] profile analysis using the JANA2000 computer program,[15] the neutron data having first been corrected for the effects of absorption. The peak shape was modeled by an asymmetry-corrected pseudo-Voigt function with, in the case of sample Q, a correction for anisotropic broadening. Magnetization measurements were made as a function of temperature using a Quantum Design MPMS SQUID magnetometer; data were collected on warming after cooling in both zero field (ZFC) and the measuring field of 100 Oe (FC). Data were also collected at selected temperatures as a function of field ($-50 \le H/kOe \le 50$) after cooling from room temperature in a field of 50 kOe.

Results

Both of the target compositions correspond to commensurately modulated structures which can be described in 3D unit cells. However, neither of the X-ray powder diffraction patterns taken from the reaction products could be indexed in a 3D unit cell, and all subsequent analysis was therefore carried out using a (3+1)D superspace model to describe these incommensurate composite structures. A structure of this type contains two subsystems, each of which exhibits approximate translational symmetry. The scattering vector, **S**, for a reflection in the diffraction pattern of such a material can be written as

$$\mathbf{S} = h\mathbf{a_1}^* + k\mathbf{a_2}^* + l\mathbf{a_3}^* + m\mathbf{a_4}^*$$

where $\mathbf{a}_n^*$ ($n = 1, 2, 3, 4$) form the basis set of reciprocal lattice vectors and h,k,l,m are integer indices. The scattering actually occurs in 3D space, and the fourth reciprocal basis vector can therefore be written as a linear combination of the other three:

$$\mathbf{a_4}^* = \alpha\mathbf{a_1}^* + \beta\mathbf{a_2}^* + \gamma\mathbf{a_3}^*$$

In the compounds under discussion, the two subsystems correspond to the chains of octahedra and prisms, the [(A′,B)O_3] system, and the chains of cations which separate them, the [A] system. The two subsystems have the lattice vectors $\mathbf{a_1}$ and $\mathbf{a_2}$ in common. The modulation vector for each system is determined by the periodicity of the other, resulting in modulation wavevectors of $\mathbf{q^1} = \mathbf{a_4}^* = \gamma\mathbf{a_3}^*$ for the first subsystem and $\mathbf{q^2} = \mathbf{a_3}^* = (1/\gamma)\mathbf{a_4}^*$ for the second subsystem. One

(11) Zakhour-Nakhl, M.; Weill, F.; Darriet, J.; Perez-Mato, J. M. *Int. J. Inorg. Mater.* **2000**, *2*, 71.
(12) Zakhour-Nakhl, M.; Claridge, J. B.; Darriet, J.; Weill, F.; zur Loye, H. C.; Perez-Mato, J. M. *J. Am. Chem. Soc.* **2000**, *122*, 1618.
(13) Stitzer, K. E.; El Abed, A.; Darriet, J.; zur Loye, H.-C. *J. Am. Chem. Soc.* **2001**, *123*, 8790.
(14) Gourdon, O.; Petricek, V.; Dusek, M.; Bezdicka, P.; Durovic, S.; Gyepesova, D.; Evain, M. *Acta Crystallogr.* **1999**, *B55*, 841.
(15) Petricek, V.; Dusek, M. *The Crystallographic Computing System JANA2000*; Institute of Physics: Praha, Czech Republic, 2000.
(16) Dusek, M.; Petricek, V.; Wunschel, M.; Dinnebier, R. E.; van Smaalen, S. *J. Appl. Crystallogr.* **2001**, *34*, 398.
(17) El Ahmed, A.; Gaudin, E.; Zur-Loye, H. C.; Darriet, J. *Solid State Sci.* **2003**, *5*, 59.
(18) Blake, G. R.; Sloan, J.; Vente, J. F.; Battle, P. D. *Chem. Mater.* **1998**, *10*, 3536.
(19) Rietveld, H. M. *J. Appl. Crystallogr.* **1969**, *2*, 65.

system, conventionally [(A′,B)O_3] is taken as the reference system, with the superspace group $R3m(00\gamma)0s$; $\mathbf{a_1}$, $\mathbf{a_2}$, and $\mathbf{a_3}$ (x_1, x_2, x_3) are thus analogous to the 3D parameters **a**, **b**, **c** (x, y, z) for this subsystem. The compound is commensurate (incommensurate) when γ is rational (irrational), and the composition and the modulation vector can be shown[9,10] to be linked by the relationship $\gamma = (1 + x)/2$. In this superspace formalism, all the oxide sites within the unit cell are generated from a single position, (x_1, x_2, x_3) = ($\sim^1/_6$, $\sim^1/_6$, $^1/_2$); the sequence of octahedral and prismatic interstices is generated by the symmetry operators of the superspace group, together with an occupation modulation function (a Crenel function along $\mathbf{a_4}$, centered at $x_4 = {}^1/_4$ with a width $\Delta = {}^1/_2$). To distinguish between the heights of the octahedra and prisms, a displacive *z*-modulation must be introduced. The simplest function which can combine this displacement with the Crenel-like site variation is a sawtooth function parametrized by Δ, x_4, and δ_O; δ_O is the maximum amplitude of the sawtooth function along *z*. The modulation parameters for the cations can be related to those which describe the oxide ion through simple geometrical considerations. The octahedral (B) and prismatic sites (A′) are described by a single average position modulated by appropriate sawtooth functions ($\Delta_{A'} = \gamma - {}^1/_2$, $\Delta_B = 1 - \gamma$, centered on $x_{4,A'} = {}^1/_4$ and $x_{4,B} = 0$ with displacive amplitudes along *z* of $\delta_{A'} = x\delta_O$, $\delta_B = (1 - x)\delta_O$). The second subsystem, the [A] sublattice, is described in the superspace group $P\bar{3}c1(00(1/\gamma))$. A single cation site at ($\sim^1/_3$, 0, $^1/_4$) produces two types of A cations, those (Sr1) which do not lie at the same height as the trigonal prismatic sites, and those (Sr2) which do. Again, sawtooth functions ($\Delta_{Sr1} = (1 - 2x)/3(1 + x)$, $x_{4,Sr1} = {}^1/_2$, $\delta_{Sr1} = (1 - 2x)\delta_{Sr2}/3x$ and $\Delta_{Sr2} = x/1 + x$, $x_{4,Sr2} = 0$, $\delta_{Sr2} = -(x/4)(1 - 2|\delta_O|(1 - x))$ are used to determine the occupation and displacement of sites at a particular height in the unit cell. It is possible, for sites in either subsystem, to introduce additional harmonic functions in order to improve the modeling of atomic displacements along x_3, and, for the oxide ions and the Sr^{2+} cations, in the x_1x_2 plane. Thus the formalism needed to describe a structure in (3+1)D superspace is more complex than that needed to describe a conventional 3D structure, but the number of independent parameters to be refined during structure analysis is lower.

Refinement of the structures of samples P and Q against X-ray diffraction data proceeded smoothly using this approach when first and second order ($m = 1, 2$) satellite reflections were included in the analysis. No additional harmonic functions were introduced to model the atomic displacements. Cobalt cations were assigned to the trigonal prismatic A′ site and Mn was assigned to the octahedral B site; no attempt was made to refine this distribution because of the similar X-ray scattering factors of Mn and Co. The isotropic atomic displacement parameter at the prismatic site in sample Q refined to a negative value within one standard deviation of zero and was subsequently fixed at zero. The refined compositional and unit cell parameters are summarized in Table 1, and the observed, calculated, and difference diffraction profiles of sample P are shown in Figure 2.

Regions of the profiles containing weak Bragg peaks from the sample holder were excluded from the analysis

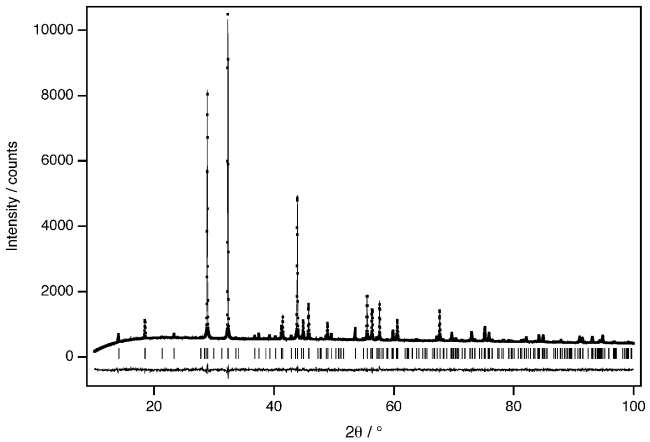

Figure 2. Observed, calculated, and difference X-ray diffraction patterns of $Sr_{1+x}(Co,Mn)O_3$, sample P. Reflection positions are marked.

Table 1. Compositional and Structural Parameters of $Sr_{1+x}(Co,Mn)O_3$ Derived from Rietveld Refinement Against X-ray Powder Diffraction Data

	sample P	sample Q
x (target)	0.2727	0.2857
γ_t (target)	0.63636	0.64286
γ_m (measured)	0.63279(2)	0.64024(3)
x_m (= $2\gamma_m - 1$)	0.26558(3)	0.28048(4)
a_1/Å	9.5838(2)	9.5845(2)
a_3/Å	2.55259(8)	2.5617(1)
R_{wp}	4.61	5.01

of the neutron diffraction data. To account for all the reflections observed from the sample it was necessary to include first, second, and third order satellites in the refinements. All atoms were constrained to have isotropic thermal parameters. That associated with the trigonal prismatic site in P refined to a negative value within a standard deviation of zero and was consequently fixed at zero. The distribution of Mn and Co across the trigonal prismatic and octahedral sites was allowed to vary, subject only to the constraint that each of the sites was fully occupied. Trial refinements showed that the oxide site was fully occupied. In the final refinements, third-order harmonic modulations were applied to improve the description of the Sr2 and O sublattices; when applied to the A′, B, and Sr1 sublattices, the appropriate coefficients refined to insignificant values. An orthogonalization procedure was used to reduce correlations between coefficients in the relevant Fourier series.[9,10,15] The fitted diffraction patterns are shown in Figure 3, and the refined structural parameters are listed in Tables 2, 3, and 4. The mean and extreme bond lengths are listed in Table 5, and the range of observed values is represented graphically as a function of the internal coordinate ($0 < t < 1$) in Figures 4 and 5.

The temperature dependence of the molar magnetic susceptibility of samples P and Q is shown in Figure 6, and the field dependence of the magnetization at 5 and 50 K is shown in Figure 7. The two compositions show very similar magnetic behavior. In each case the ZFC and FC data overlie above 13(2) K. However, the inverse susceptibility is not a linear function of temperature and could be fitted to neither a simple Curie−Weiss law nor to a Curie−Weiss law with an additional temperature-independent term. The ZFC susceptibility shows a

Table 2. Structural Parameters of $Sr_{1+x}(Co,Mn)O_3$, Sample P, Derived from Neutron Diffraction Data[a]

atom	x_1	x_2	x_3	x_4	Δ	δ	U_{iso}/Å^2
			Subsystem 1: $R\bar{3}m(00\gamma)0s$				
A′[b]	0	0	0	(1/4)	0.13260(5)	−0.0382(6)	0
B[b]	0	0	0	0	0.36740(5)	−0.104(2)	0.010(4)
O[c]	0.1561(4)	0.1561(4)	(1/2)	(1/4)	(1/2)	−0.142(2)	0.0107(8)
			Subsystem 2: $P\bar{3}c1(00(1/\gamma))$				
Sr1	0.324(1)	0	(1/4)	(1/2)	0.12371	−0.0251(2)	0.008(3)
Sr2[c]	0.3555(8)	0	(1/4)	0	0.20962	−0.0426(4)	0.006(3)

[a] $a_1 = 9.583(1)$, $a_3 = 2.5518(3)$ Å; $\gamma = 0.63261(5)$; $R_{wp} = 6.76\%$. [b] Fractional occupancy by Co: A′ 0.71(3), B 0.08(4). [c] See also Table 4.

Table 3. Structural Parameters of $Sr_{1+x}(Co,Mn)O_3$, Sample Q, Derived from Neutron Diffraction Data[a]

atom	x_1	x_2	x_3	x_4	Δ	δ	U_{iso}/Å^2
			Subsystem 1: $R\bar{3}m(00\gamma)0s$				
A′[b]	0	0	0	(1/4)	0.14002(6)	−0.0390(6)	0.09(9)
B[b]	0	0	0	0	0.35998(6)	−0.100(1)	0.009(4)
O[c]	0.1560(4)	0.1560(4)	(1/2)	(1/4)	(1/2)	−0.139(2)	0.0115(9)
			Subsystem 2: $P\bar{3}c1(00(1/\gamma))$				
Sr1	0.325(1)	0	(1/4)	(1/2)	0.11146	−0.0231(2)	0.003(3)
Sr2[c]	0.358(1)	0	(1/4)	0	0.21869	−0.0455(4)	0.013(3)

[a] $a_1 = 9.586(1)$, $a_3 = 2.5613(5)$ Å; $\gamma = 0.64001(6)$; $R_{wp} = 6.76\%$. [b] Fractional occupancy by Co: A′ 0.78(6), B 0.10(2). [c] See also Table 4.

Table 4. Third-Order Harmonic Modulation Parameters ($u_{i,3}$; $i = 1, 2, 3$) for $Sr_{1+x}(Co,Mn)O_3$

	sample P			sample Q		
atom	$u_{1,3}$	$u_{2,3}$	$u_{3,3}$	$u_{1,3}$	$u_{2,3}$	$u_{3,3}$
O	−0.0050(4)	0.0050(4)	−0.005(3)	−0.0044(4)	0.0044(4)	−0.001(3)
Sr2	−0.002(2)	−0.005(4)	0.022(6)	0.002(1)	0.005(3)	−0.032(4)

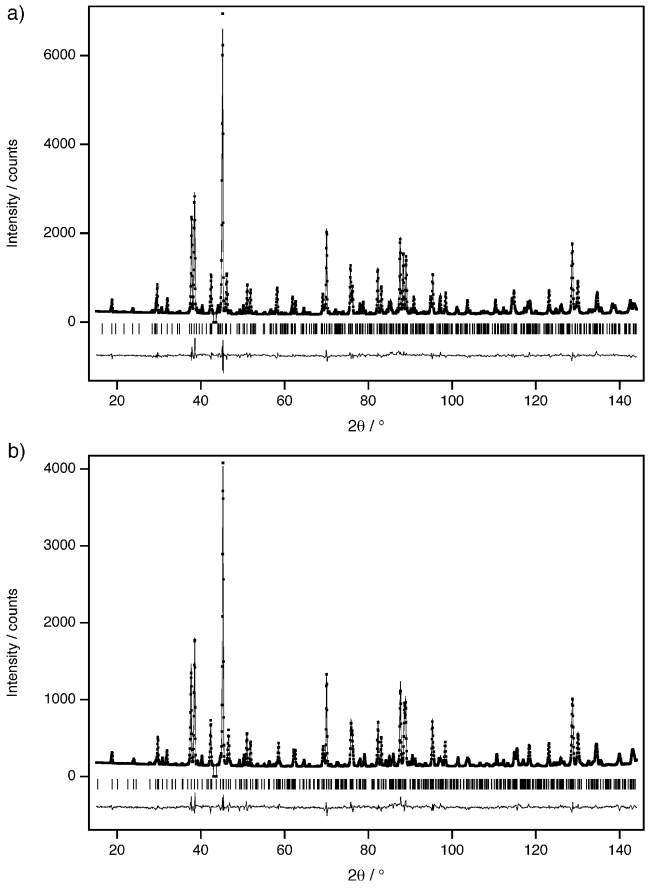

Figure 3. Observed, calculated, and difference neutron diffraction patterns of $Sr_{1+x}(Co,Mn)O_3$ (a) sample P and (b) sample Q. Reflection positions are marked.

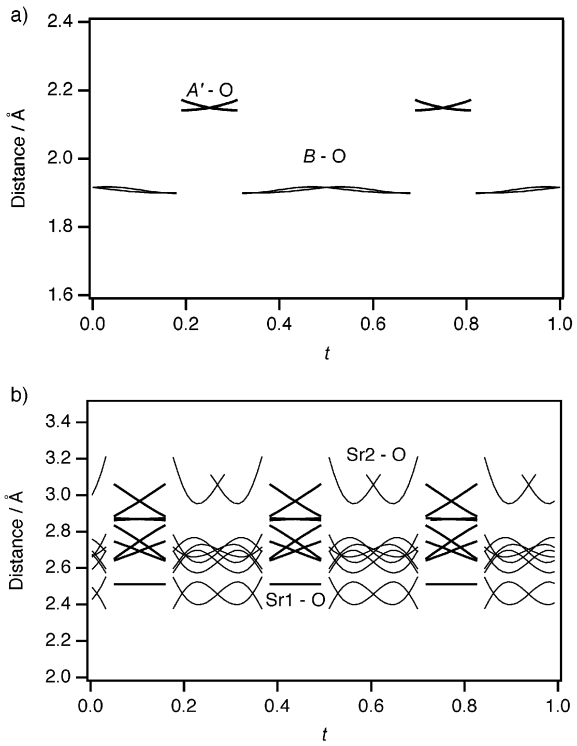

Figure 4. Variation of bond lengths in $Sr_{1+x}(Co,Mn)O_3$, sample P.

maximum at 13 K, below which temperature hysteresis is apparent between the ZFC and FC data. The magnetization is a linear function of applied field at 50 K, and the M(H) loops collected at 5 K are symmetrical about the origin.

Discussion

Two compositions in what was previously described as the incommensurate hexagonal phase of $SrCo_xMn_{1-x}O_3$ have been prepared and structurally characterized. The structures contain chains of polyhedra in which trigonal prisms are separated from each other by both dimers and trimers of face-sharing octahedra. Although the target compositions corresponded to the commensurate supercells drawn in Figure 1, the two samples both exhibit incommensurate diffraction patterns. In view of

Table 5. Refined Bond Distances (Å) for $Sr_{1+x}(Co,Mn)O_3$

	Sample P			Sample Q		
	min	max	mean	min	max	mean
A′−O	2.14(2)	2.17(2)	2.15(2)	2.14(2)	2.16(2)	2.15(2)
B−O	1.90(2)	1.92(2)	1.91(2)	1.91(2)	1.91(2)	1.91(2)
A′−B			2.721(3)			2.718(2)
B−B			2.360(2)			2.362(2)
Sr1−O	2.51(3)	3.07(2)		2.51(3)	3.02(2)	
Sr2−O	2.40(7)	3.28(9)		2.38(6)	3.22(7)	

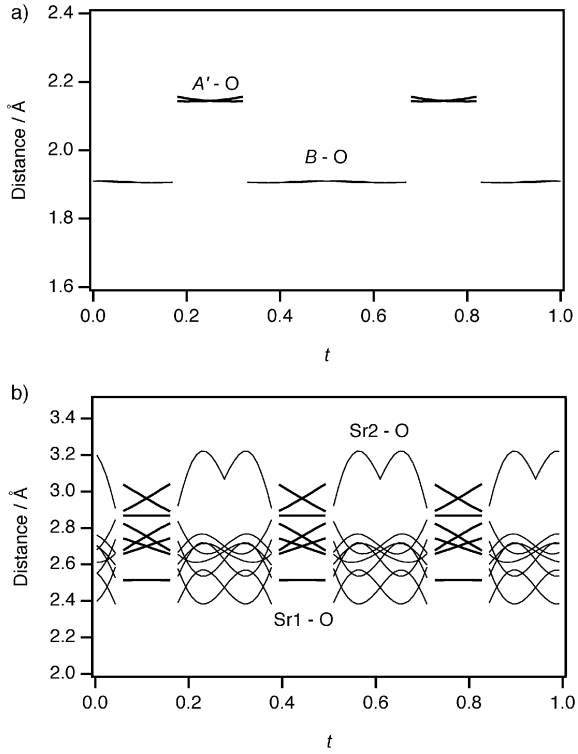

Figure 5. Variation of bond lengths in $Sr_{1+x}(Co,Mn)O_3$, sample Q.

the relationship between the modulation vector and the composition of these phases, this must mean that the principal phases in samples P and Q do not have the intended stoichiometry, although the deviation is small (Table 1); no second phase was observed in the X-ray or neutron diffraction data. Other groups have reported similar problems in controlling the composition of these phases.[17,20−22] The unit cell parameter a_1, determined in both samples by the interionic distances in an Sr_3O_9 plane, does not vary significantly between P and Q, whereas the unit cell parameter a_3, a measure of the average cation separation within the chains of polyhedra, is predictably larger for sample Q, which contains a higher proportion of the relatively large trigonal prisms. The fact that the observed γ values are lower than the target values suggests that both of our samples contain a lower fraction of trigonal prisms than was intended. The markedly different neutron scattering lengths of Mn and Co allowed us to investigate whether the two cations are completely ordered over the octahedral and prismatic sites. The data in Tables 2 and 3

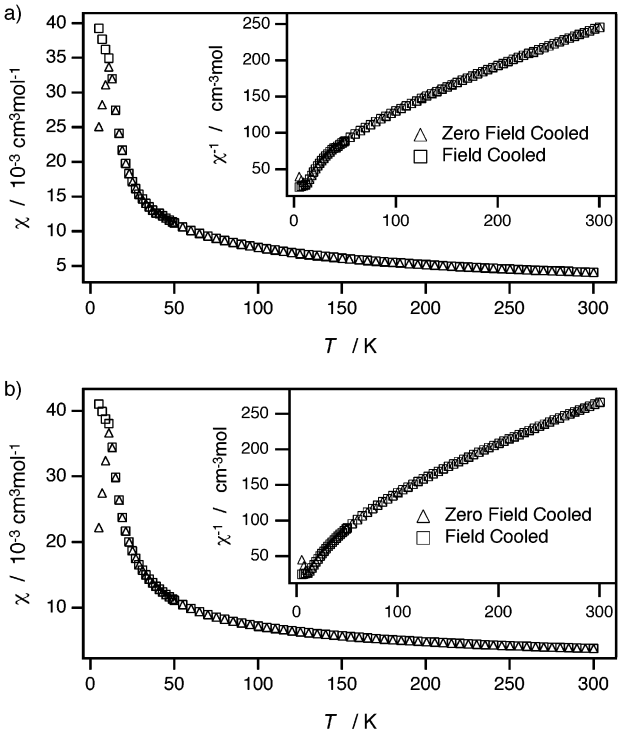

Figure 6. Temperature dependence of the molar magnetic susceptibility of $Sr_{1+x}(Co,Mn)O_3$ (a) sample P and (b) sample Q in a field of 100 Oe.

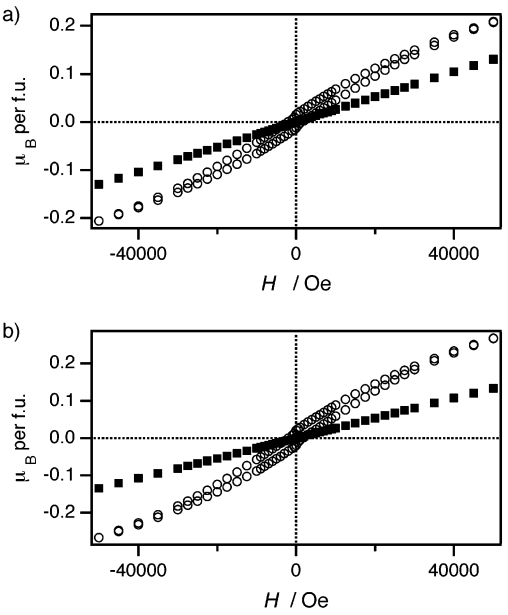

Figure 7. Field dependence of the magnetization of $Sr_{1+x}(Co,Mn)O_3$ (a) sample P and (b) sample Q at 50 K (■) and 5 K(○).

suggest that in both samples a significant fraction of the prismatic sites (∼25%) are occupied by Mn, and that in sample Q (but not sample P) there is a small but significant concentration of Co on the octahedral sites. The chemical formula could therefore be written $Sr_{1+x}(Co_{x-y}Mn_y)[Co_zMn_{1-x-z}]O_3$. However, the low precision with which y and z can be determined (see Tables 2 and 3) limits the use of this analysis in determining the composition of the sample, particularly when the thermal parameter of the prismatic site has been held fixed during the refinements. We are therefore unable to detect unambiguously a deviation from the target Mn/

(20) Bazuev, G. V.; Krasil'nikov, V. N.; Kellerman, D. G. *J. Alloys Compd.* **2003**, *352*, 190.
(21) El Abed, A.; Gaudin, E.; Lemaux, S.; Darriet, J. *Solid State Sci.* **2001**, *3*, 887.
(22) Stitzer, K. E.; Henley, W. H.; Claridge, J. B.; zur Loye, H.-C.; Layland, R. C. *J. Solid State Chem.* **2002**, *164*, 220.

Co ratio in our crystalline reaction product; the ideal value and the refined value lie within the standard deviation of the latter. Similar site disorder between the octahedral and trigonal prismatic interstices has been reported in neutron diffraction studies of other Mn-containing compounds in this family, including $Ba_6ZnMn_4O_{15}$[23] and Ca_3NiMnO_6.[24] As a result of the incommensurate nature of the sample, Figure 1 can only be a good, rather than a perfect, representation of the polyhedral sequence. Indeed, it is difficult to represent such a structure clearly using either diagrams or tables and Figure 5 perhaps gives the most useful chemical information about the structure. The Co−O bond lengths around the prismatic site (Table 5) are somewhat longer than those in $Sr_6Co_5O_{15}$ (1.973(3) Å[6]), $Sr_{14}Co_{11}O_{33}$ (2.05 Å[14]), and $Ca_3Co_2O_6$ (2.062 Å[25]), but comparable to those in $Ba_8CoRh_6O_{21}$ (2.184(1) − 2.197(1) Å[26]). On the basis of a comparison with a coordination complex,[27] the prismatic Co in $Sr_{14}Co_{11}O_{33}$ has been assigned as Co^{2+}, as has that in $Ba_8CoRh_6O_{21}$ although zur Loye et al comment that the bonds in the latter are longer than might be expected for Co^{2+} on the basis of bond-valence calculations; they and others make it clear that some ambiguity remains. The limited evidence available thus suggests that the relatively long bonds observed around the trigonal sites in samples P and Q are likely to involve Co^{2+}; the presence of Mn^{2+} on a fraction of these sites would raise the average bond length above that expected from Co^{2+} alone, although Mn^{2+} is not usually observed in samples prepared as these were. In the case of the target stoichiometries $Sr_{14}Co_3Mn_8O_{33}$ and $Sr_9Co_2Mn_5O_{21}$, if all the Co is divalent then the Mn is expected to be present as Mn^{4+}. The mean B−O distances (Table 5) are very similar to the mean Mn−O bond length in $SrMnO_3$ [28] and $Ba_4Mn_3O_{10}$,[29] both of which contain Mn^{4+} in face sharing octahedra; the B−B distance (2.36 Å) is significantly shorter than those in both $SrMnO_3$ (2.50 Å) and $Ba_4Mn_3O_{10}$ (2.55 Å), although an equally short distance has been observed in $Sr_6Co_5O_{15}$ using single-crystal X-ray diffraction. The A′−B distance (2.721 Å) is long compared to the values determined in single-crystal X-ray studies of $Sr_6Co_5O_{15}$ and $Sr_{14}Co_{11}O_{33}$, the latter having been analyzed using a 4D model which included additional harmonic modulations. The B−B distance determined by neutron powder diffraction is also shorter than that deduced in the original EXAFS study[1] of the $Sr(Co,Mn)O_3$ system (∼2.5 Å), although the A′−B distance, originally ascribed to the presence of edge-sharing octahedra, was previously measured to be 2.87 Å. The range of Sr−O distances found in the present study is typical of those found in mixed-metal oxides.

The data presented in Figures 6 and 7 show that both samples are paramagnetic at 50 K, but that they undergo a magnetic transition at 13(2) K. The deviation from Curie−Weiss behavior shows that intercation superexchange interactions are strong well above this temperature. Those between Mn cations in face-sharing octahedra are known to be significant at 300 K[28] and the A′−B distance is short enough to facilitate strong coupling between the octahedral and prismatic sites. The behavior of the susceptibility at 13 K suggests that the low-temperature phase is either a canted antiferromagnet or a spin glass with entropic spin clusters[30] present to cause the continued increase in the FC susceptibility on further cooling. The absence of any vertical displacement of the hysteresis loops in Figure 7 is consistent with the adoption of a canted antiferromagnetic structure, although the lack of a sharp increase in the FC susceptibility at 13 K is more suggestive of a spin glass phase. The frustration needed to cause glass formation could arise from the disordered nature of the Co/Mn distribution, or from competition between intrachain and interchain superexchange interactions. These questions will have to wait for an answer until we can refine the magnetic structure of a modulated phase from powder diffraction data. It is interesting to note that the magnetic properties of the related phases $Sr_3NiRhO_{6+\delta}$, $Sr_3CuRhO_{6+\delta}$,[22] $Sr_{4/3}(Mn_{2/3}Ni_{1/3})O_3$,[31] and $Ca_3Co_{1+x}Mn_{1-x}O_6$[32] have been shown to be very sensitive to disorder and structural modulation. The most closely related system studied to date, $Ca_3Co_{1+x}Mn_{1-x}O_6$, shows susceptibility maxima at 18 and 13 K for $x = 0.25$ and $x = 0$, with hysteresis apparent below the susceptibility maximum of the disordered ($x = 0.25$) composition. No magnetic Bragg peaks were observed in the case of the $x = 0$ sample at 4.2 K.

To conclude, we have demonstrated that the incommensurate hexagonal phase identified previously in the Sr−Co−Mn−O system is a member of the $A_{1+x}A'_xB_{1-x}O_3$ family of incommensurate modulated structures. We have been able to refine the structures of two compositions by applying the (3+1)D superspace formalism in the analysis of neutron powder diffraction data, with the contrasting neutron scattering lengths of Mn and Co allowing us to investigate the cation distribution over the octahedral and prismatic sites. We are not aware of any previous studies of incommensurately modulated structures by profile analysis of neutron powder diffraction data. However, the quality of the fit shown in Figure 3 is good, and it is based on a chemically reasonable structural model (Table 5). The magnetic susceptibility of both samples shows a transition at 13 K, although it has not yet been possible to determine the exact nature of the low-temperature magnetic phase.

Acknowledgment. We are grateful to EPSRC for financial support, and to Thomas Hansen for experimental assistance at ILL Grenoble.

CM031096+

(23) Cussen, E. J.; Vente, J. F.; Battle, P. D. *J. Am. Chem. Soc.* **1999**, *121*, 3958.
(24) Bazuev, G. V.; Zubkov, V. G.; Berger, I. F.; Arbuzova, T. I. *Solid State Sci.* **1999**, *1*, 365.
(25) Fjellvåg, H.; Gulbrandsen, E.; Aasland, S.; Olsen, A.; Hauback, B. C. *J. Solid State Chem.* **1996**, *124*, 190.
(26) zur Loye, H.-C.; Stitzer, K. E.; Smith, M. D.; El Abed, A.; Darriet, J. *Inorg. Chem.* **2001**, *40*, 5152.
(27) Bertrand, J. A.; Kelly, J. A.; Vassian, E. G. *J. Am. Chem. Soc.* **1969**, *91*, 2394.
(28) Battle, P. D.; Gibb, T. C.; Jones, C. W. *J. Solid State Chem.* **1988**, *74*, 60.
(29) Zubkov, V. G.; Tyutyunnik, A. P.; Berger, I. F.; Voronin, V. I.; Bazuev, G. V.; Moore, C. A.; Battle, P. D. *J. Solid State Chem.* **2002**, *167*, 453.
(30) Fiorani, D.; Viticoli, S.; Dormann, J. L.; Tholence, J. L.; Murani, A. P. *Phys. Rev. B* **1984**, *30*, 2776.
(31) El Abed, A.; Gaudin, E.; Darriet, J.; Whangbo, M.-H. *J. Solid State Chem.* **2002**, *163*, 513.
(32) Zubkov, V. G.; Bazuev, G. V.; Tyutyunnik, A. P.; Berger, I. F. *J. Solid State Chem.* **2001**, *160*, 293.